

ORIGINAL ARTICLE

Microglia: An Intrinsic Component of the Proliferative Zones in the Fetal Rhesus Monkey (*Macaca mulatta*) Cerebral Cortex

Nicole Barger¹, Janet Keiter², Anna Kreutz², Anjana Krishnamurthy¹, Cody Weidenthaler², Verónica Martínez-Cerdeño^{3,4,8}, Alice F. Tarantal^{5,6,7} and Stephen C. Noctor^{1,8}

¹Department of Psychiatry and Behavioral Sciences, School of Medicine, UC Davis, Sacramento, CA 95817, USA, ²Neuroscience Graduate Program, UC Davis, Davis, CA 95616, USA, ³Department of Pathology and Laboratory Medicine, School of Medicine, UC Davis, Sacramento, CA 95817, USA, ⁴Institute for Pediatric Regenerative Medicine and Shriners Hospitals for Children Northern California, Sacramento, CA 95817, USA, ⁵Department of Pediatrics, School of Medicine, UC Davis, Sacramento, CA 95817, USA, ⁶Department of Cell Biology and Human Anatomy, School of Medicine, UC Davis, Davis, CA 95616, USA, ⁷California National Primate Research Center and Center for Fetal Monkey Gene Transfer for Heart, Lung, and Blood Diseases, UC Davis, Davis, CA 95616, USA and ⁸MIND Institute, School of Medicine, UC Davis, Sacramento, CA 95817, USA

Address correspondence to Stephen C. Noctor, UC Davis MIND Institute, 2805 50th Street, Sacramento, CA 95817, USA. Email: scnoctor@ucdavis.edu

Abstract

Microglial cells are increasingly recognized as modulators of brain development. We previously showed that microglia colonize the cortical proliferative zones in the prenatal brain and regulate the number of precursor cells through phagocytosis. To better define cellular interactions between microglia and proliferative cells, we performed lentiviral vector-mediated intraventricular gene transfer to induce enhanced green fluorescent protein expression in fetal cerebrocortical cells. Tissues were collected and counterstained with cell-specific markers to label microglial cells and identify other cortical cell types. We found that microglial cells intimately interact with the radial glial scaffold and make extensive contacts with neural precursor cells throughout the proliferative zones, particularly in the rhesus monkey fetus when compared to rodents. We also identify a subtype of microglia, which we term ‘periventricular microglia’, that interact closely with mitotic precursor cells in the ventricular zone. Our data suggest that microglia are structural modulators that facilitate remodeling of the proliferative zones as precursor cells migrate away from the ventricle and may facilitate the delamination of precursor cells. Taken together, these results indicate that microglial cells are an integral component of cortical proliferative zones and contribute to the interactive milieu in which cortical precursor cells function.

Key words: cortical development, microglial cells, proliferative zones, radial glial cells, rhesus monkey

Introduction

The developing cerebral cortex forms from the proliferative output of precursor cells located in the ventricular zone (VZ)

and subventricular zones (SVZ). While the cellular composition of the cortical proliferative zones has been examined in great detail for over a century, recent advances have uncovered

important factors that regulate the function of neural precursor cells (NPC). Fluorescent reporter gene labeling of cells in the developing brain over the past 2 decades has increased the pace of discovery and greatly expanded our understanding of NPC function and regulation at the molecular, cellular, and structural levels. Nevertheless, our understanding of cellular interactions in the proliferative zones remains incomplete.

Microglial cells, the innate immune cell of the central nervous system (CNS) are now recognized as key players in CNS development. Microglia have been shown to participate in a variety of developmental programs including the establishment of axonal pathways (Squarzoni et al. 2014), synapse development and maintenance (Paolicelli et al. 2011; Schafer et al. 2012), cortical layer formation (Ueno et al. 2013; Squarzoni et al. 2014), and an array of other processes (Salter and Stevens 2017). Microglial cells in the embryonic mouse brain have been shown to arise from myeloid precursor cells in the yolk sac (Alliot et al. 1999; Ginhoux et al. 2010) and migrate into the cerebral cortex during very early stages of cell genesis. Microglia begin to colonize the cortex in the mouse by embryonic day (E) 11.5 (Swinnen et al. 2013; Arno et al. 2014), in the rat by E13 (Cunningham et al. 2013b), in the rhesus (Cunningham et al. 2013b) and cynomolgus monkey (Toyoshima et al. 2012) during the first trimester (prior to 50 days gestation), and in the human cerebrum by 6 weeks of gestation (Andjelkovic et al. 1998; Verney et al. 2010). In each species, microglial cells do not initially spread widely throughout the brain, as found in the mature brain, but distribute to specific regions and laminae of the brain that include the cortical proliferative zones (Rezaie and Male 1999; Swinnen et al. 2013; Cunningham et al. 2013b; Arno et al. 2014). We previously showed that microglial cells contribute to the regulation of cell production in the developing cerebral cortex by phagocytosing NPCs in the VZ and SVZ, particularly in rhesus monkeys. We used markers for the cell-specific nuclear transcription factors Pax6 and Tbr2 to identify NPC nuclei and Iba1 to label microglial cells (Cunningham et al. 2013b). This approach provided clear evidence of cell contact, envelopment, and phagocytosis of NPC nuclei by microglia in the fetal cerebral cortex. To better understand cellular interactions between microglia and NPCs prior to phagocytosis, and the cellular interactions that occur between microglia and NPCs that do not involve or culminate in phagocytosis, we labeled NPCs with enhanced green fluorescent protein (eGFP) via in utero lentiviral vector-mediated intraventricular injections in rats and under ultrasound guidance in rhesus monkeys. This approach fully labeled the cell body and processes of NPCs with fluorescent reporter gene and provided a means to further establish the range, frequency, and characteristics of microglial interactions with NPCs in the cortical proliferative zones, broadening our understanding of microglial functions with relation to proliferative cells in the developing brain.

The results of these studies provide a novel perspective on microglial function in the prenatal cerebral cortex. We show that microglial cells are an intrinsic component of the cortical proliferative zones that make extensive contacts with NPCs. In addition, microglia closely interact with radial glial (RG) cells and intermediate progenitor (IP) cells in the VZ, and RG pial fibers and migrating precursor cells in the SVZ. Furthermore, we also show that microglial cells can “multitask,” with individual microglia simultaneously contacting, enveloping, and phagocytosing multiple NPCs. We provide evidence for a unique subset of microglial cells that appear in the VZ near the margin of lateral ventricle during later stages of cortical neurogenesis. These periventricular microglia interact closely with precursor cells undergoing division at the ventricle at a time when many RG cells and newborn

daughter cells delaminate and migrate away from the ventricle toward the overlying SVZ. We found that microglial cells contact NPCs in both rat and rhesus monkey developing cerebral cortex, but that microglial cell density is substantially greater in fetal rhesus proliferative zones. Together, these findings demonstrate that microglial cells contribute to the cell-dense, highly interactive milieu in the prenatal cortical proliferative zones.

Materials and Methods

Preparation of Viral Vectors

Retrovirus

Replication-incompetent pantropic retrovirus for use in rats and that encodes eGFP was prepared as described previously (Noctor et al. 2001). 293gp NIT-GFP cells were transiently transfected with pVSV-G (Clontech) using Lipofectamine 2000 (Invitrogen) to pseudotype viral particles. Supernatant was collected at 48 h post-transfection and virus concentrated by centrifugation at 50 000 × g for 1.5 h at 4 °C, resuspended in Opti-MEM (Invitrogen), and stored at ≤−80 °C until use.

HIV-1-Derived Lentiviral Vector

The HIV-1-derived lentiviral vector containing the eGFP under transcriptional control of the MND U3 long-terminal repeat was constructed as previously described (Naldini et al. 1996; Zufferey et al. 1997) and kindly provided by Dr. Donald Kohn. The CCL-lentiviral vector was used to generate recombinant lentiviral particles by transient transfection into 293 T cells using established protocols (Cooper et al. 2011).

Animals

All animal procedures conformed to the requirements of the Animal Welfare Act and protocols were approved prior to implementation by the Institutional Animal Care and Use Committee (IACUC) at the University of California, Davis.

Rat

Pregnant rats at E19 were injected as previously described (Martinez-Cerdeño et al. 2012). Briefly, rats were anesthetized with 3–5% Isoflurane, a laparotomy was performed, and the uterine horns containing embryos removed from the abdominal cavity, retrovirus was injected into the lateral ventricles of embryos, then the uterine horns were returned to the abdominal cavity and the muscular layer and skin closed with sutures. The injected embryos were harvested 1 day later, removed from the dams and transcardially perfused with 4% paraformaldehyde (PFA). Brains were extracted and postfixed in 4% PFA for 24 h, washed in phosphate buffered saline (PBS), then cryoprotected in 30% sucrose with 0.01% sodium azide for 24 h.

Rhesus Monkey

Normally cycling, adult female rhesus monkeys (*Macaca mulatta*) with a history of prior pregnancy were bred and identified as pregnant using established methods (Tarantal 2005) ($N = 4$). Pregnancy in the rhesus monkey is divided into trimesters by 55 day increments with 0–55 days gestation representing the first trimester, 56–110 days gestation representing the second trimester, and 111–165 days gestation the third trimester (term 165 ± 10 days). All fetuses were assessed sonographically to confirm normal growth and development prior to gene transfer using standardized parameters (Tarantal 2005). The dams were administered ketamine hydrochloride (10 mg/kg) intramuscular (IM) for

ultrasound examinations. On the day of gene transfer, the dams were administered telazol (5–8 mg/kg IM) and were aseptically prepared for transabdominal ultrasound-guided fetal gene delivery. A volume of ~50 μ l of the vector supernatant was injected under sterile conditions into the lateral ventricle using established methods (Chang et al. 2002) ($N = 2$ late first trimester or $N = 2$ early second trimester). Post-gene transfer sonographic assessments were performed regularly until fetal tissue harvest (either 5 or 14 days post-gene delivery) according to standardized protocols (Tarantal and Skarlatos 2012).

Tissue Processing

Rat

Rat brains were placed in OCT media (Fisher) and flash frozen in 2-methyl-butane (Sigma) on dry ice. Frozen brains were sectioned coronally at 40 or 100 μ m on a cryostat, and free-floating sections stored in PBS with 0.01% sodium azide at 4 °C.

Rhesus Monkey

Fetal brains were harvested 5 or 14 days post-gene transfer. Tissues were either perfused or immersion-fixed with 4% paraformaldehyde (PFA) for 2–3 days. The right hemisphere was cryoprotected in 30% sucrose in preparation for cryosectioning. All tissues were cryosectioned at 100 μ m on a sliding microtome.

Rat Immunohistochemistry

Free-floating tissue was washed 2 \times in PBS, blocked with 10% donkey serum, then 1% Triton-x in PBS for 1 h at room temperature. Tissue was incubated in primary antibody, goat anti-Iba1 (Wako, 1:500), which was diluted in 2% donkey serum with 0.2% Triton-x in PBS and incubated for up to 3 days at 4 °C on a rocking platform. Tissue was washed 3 \times in PBS, before incubating in secondary antibody (donkey anti-goat, Jackson ImmunoResearch, 1:500) diluted in 2% donkey serum with 0.2% Triton-x in PBS and was incubated for 2 h at room temperature on a rocking platform. Tissue was stained with DAPI (Sigma, 1:1000) in PBS for 15 min followed by 2 \times PBS washes. Tissue was then mounted on SuperFrost slides (Fisher), covered with Mowiol, and coverslipped.

Rhesus Monkey Immunohistochemistry

Control specimens were mounted on slides, submerged in 10 mM Citrate Buffer (Fisher), pH 6, and heated in a steamer for 15 min (modification of Tang et al. 2007). Tissues expressing eGFP were heated at 37 °C for 30 min in 10 mM citrate buffer, pH 3.5. After the citrate buffer reached room temperature, sections were rinsed 3 times for 5 min and incubated in a blocking buffer, containing 10% donkey serum (Millipore) and 1% Triton X-100 (Acros) for 1.5 h at room temperature. Sections were then incubated for 2–3 days in a primary antibody buffer containing 2% donkey serum, 1% Triton X-100, and antibodies including some combination of sheep anti-EOMES (1:150, R&D Systems, AF6166), mouse antiphosphorylated vimentin / 4a4 (1:100; MBL, D076-3), rabbit anti-Pax6 (1:100, Abcam), rabbit anti-Tbr2 (1:100, Abcam, ab23345), goat anti-GFAP (1:50, Santa Cruz), goat anti-Iba1 (1:200, Abcam, ab5076), or chicken anti-Iba1 (1:150, SySy, 234 006). Sections were then rinsed and incubated for 2 h at room temperature in a secondary antibody buffer with 2% donkey serum and 1% Triton X-100 which included donkey anti-mouse, donkey anti-rabbit, donkey anti-chicken, donkey anti-goat, or donkey anti-sheep conjugated to the fluorophores AF405, AF488, TRITC, or AF647. All secondary antibodies were used at a concentration of 1:250 (Jackson ImmunoResearch).

After secondary incubation, the sections were rinsed in PBS and a coverslip placed with Mowiol.

Data Collection

Sections were imaged on an Olympus Fluoview 1000 confocal microscope equipped with 405, 488, 543, and 633 laser lines. Image stacks were acquired at 0.5–1.5 μ m steps using 100 \times (NA, 1.3) or 60 \times (NA, 1.4) objectives. Observations were based on over 200 confocal image stacks collected from cortical regions spanning the rostro-caudal expanse of the fetal brain. Cellular density estimate of microglia in the inner SVZ (iSVZ) was performed in 100- μ m thick coronal sections of the occipital lobe collected from E20 rats and 100 days gestation fetal rhesus monkeys. A grid of 100 \times 100 μ m was overlaid on the Z-stack within Fluoview and all microglial cell bodies that fell within the grid through the Z-stack were counted. Data were normalized to 100 μ m³ for Z-series that did not encompass a full Z-depth of 100 μ m.

Results

We have previously shown that microglial cells phagocytose NPCs in the developing cerebral cortex (Cunningham et al. 2013b). In this previously published study, we identified NPCs by immunostaining with cell-specific nuclear transcription factors such as Pax6 or Tbr2, and labeled microglial cells with anti-Iba1 antibodies to show that Pax6+ and Tbr2+ NPC nuclei were enveloped and phagocytosed by microglia in the cortical proliferative zones (Cunningham et al. 2013b). To better define interactions between fetal microglia, NPCs, and other cell types in the developing cortex, we performed fetal intraventricular injections with a retroviral vector (Noctor et al. 2008) in the E19 rat to label the entire cell body and processes of NPCs with eGFP and counterstained tissue with anti-Iba1 antibodies to label microglial cells (Imai et al. 1996).

Rat Microglial Cells Contact NPCs in the Developing Cerebral Cortex

Intraventricular injections were performed on E19 rats, and brain tissue harvested 1 day later on E20. Tissue was processed and immunostained with Iba1 to label microglial cells and imaged on a confocal microscope. We observed close contact between microglia and eGFP-labeled precursor cells. Microglia contacted, and in some cases, enveloped cellular processes of eGFP-labeled RG cells (Fig. 1A). We also noted examples of eGFP+ cells in the VZ with multiple processes that contacted nearby microglial cells (Fig. 1B).

We next assessed cellular interactions between microglial cells and NPCs in control rat embryos that had not been injected with retrovirus. Rat neocortical tissue was coimmunostained with 4a4 antibodies against phosphorylated vimentin to label M-phase dividing precursor cells in the VZ and SVZ (Kamei et al. 1998; Noctor et al. 2002; Cunningham et al. 2013a), and against Iba1 to label microglia. We noted that Iba1+ microglial cells in the VZ extended processes that contacted dividing precursor cells undergoing division at the ventricular surface (Fig. 1C), and away from the lateral ventricle (Fig. 1D–F). The microglia contacted both the soma and pial process of the dividing precursor cells (Fig. 1G), confirming that these interactions occur in the normally developing brain.

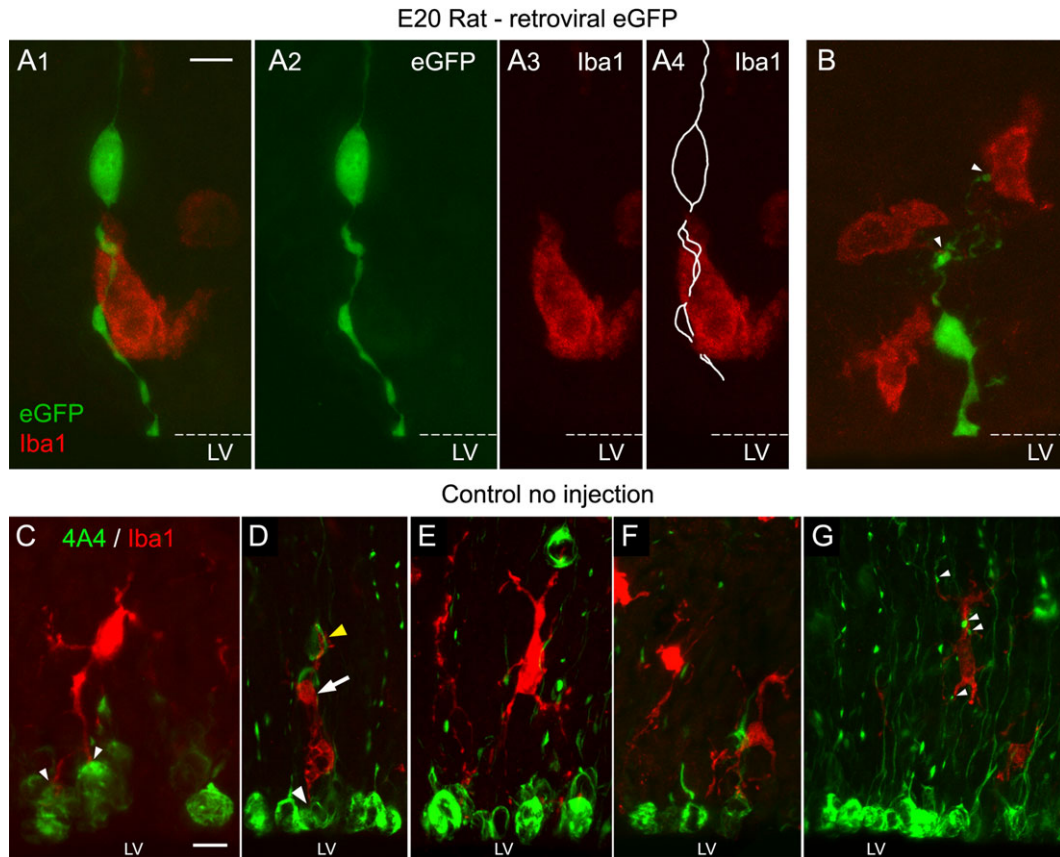


Figure 1. Microglial cells contact eGFP-expressing RG cells in the VZ of the embryonic day (E) 20 rat. (A₁-A₄) The ventricular contacting process of an RG cell (green) in the VZ is intimately surrounded by an Iba1+ microglial cell (red), forming a groove through which the RG cell processes course. White line highlights trajectory of RG cell process through the microglial cell. (B) An eGFP-expressing RG cell (green) contacted multiple microglia (red) in the VZ (white arrowheads). (C) Microglial cells contact mitotic precursor cells in control rat cerebral cortex. An Iba1+ microglial cell (red) extended a process toward the ventricular surface that bifurcated and terminated on 2 4a4+ M-phase dividing precursor cells (green, white arrowheads). (D) An Iba1+ microglia (red, white arrow) extended a process containing apparent lysosomes toward the ventricle that contacted 4a4+ cells (white arrowhead). The same microglia extended a second process in the opposite direction that contacted a precursor cell dividing away from the ventricle (yellow arrowhead). (E-G) Iba1+ microglia (red) in the VZ extended processes toward the ventricle that intercalate between dividing precursor cells (green). Iba1+ microglia (red) in the SVZ made direct contact with and enveloped the varicosities (white arrowheads) on pial fibers of M-phase dividing RG cells. LV, lateral ventricle. Scale bars = 10 μm .

Density of Microglial Cells is Higher in Fetal Rhesus Monkey Cortex Compared to Rat

We compared microglial distribution in the embryonic rat with that in fetal rhesus monkey at the same relative stage of cortical neurogenesis and found that the density of microglia in the proliferative zones of the fetal rhesus monkey was substantially higher than in the embryonic rat cortex (Fig. 2).

The morphology of individual microglial cells could be readily discerned in the embryonic rat proliferative zones (Fig. 2C-E), but the density of microglial cells was often too high to discern individual microglia in the proliferative zones of some regions of the fetal rhesus monkey cortex (Fig. 2D, Supplementary Movies 1 and 2). A comparison of microglial numbers in the occipital lobe of prenatal monkey versus rat showed that the density of microglia in the iSVZ was higher in rhesus monkeys ($86.4 \pm 14.8^{\text{SEM}}$ per $100 \mu\text{m}^3$) than in rats at the same stage of development ($6.6 \pm 0.9^{\text{SEM}}$ per $100 \mu\text{m}^3$).

Given the increased density of microglial cells in the proliferative zones of rhesus monkey cortex, the large difference in the size of the proliferative zones between rat and rhesus monkey (Martinez-Cerdeño et al. 2012) and the close phylogenetic and developmental relationship to humans, we focused these

studies on fetal rhesus monkey cerebral cortex that had been injected with a lentiviral vector expressing eGFP under ultrasound guidance. Direct injections into the lateral ventricle were performed during the second trimester (80 days gestation) when upper layer cortical neurons were being generated in the fetal monkey cerebral cortex (Rakic 1974). Cortical tissue was harvested 5 or 14 days postinjection, sectioned, and immunostained. We used a cocktail of 3 markers including Pax6 to identify RG cells, Tbr2 to label IP cells, Iba1 to label microglia, GFAP to label RG cell bodies and pial fibers, 4a4 to identify M-phase precursor cells, and DAPI to label nuclei. Sections were imaged with a confocal microscope to record the eGFP+ lentiviral labeled cells and 3 additional markers (Fig. 3).

Strong eGFP expression was observed in cortical cells lining the lateral ventricle. EGFP+ cells included RG cells, IP cells, and microglia. In $100 \mu\text{m}$ thick coronal sections, we were able to visualize eGFP+ RG cells with pial fibers that coursed hundreds of microns toward the overlying cortical plate (Fig. 3A).

Microglia Contact RG Cells in Fetal Rhesus Monkey Cortex

EGFP+ RG cells were contacted by multiple microglia in the VZ and along the pial fiber in the SVZ. The RG cell shown in

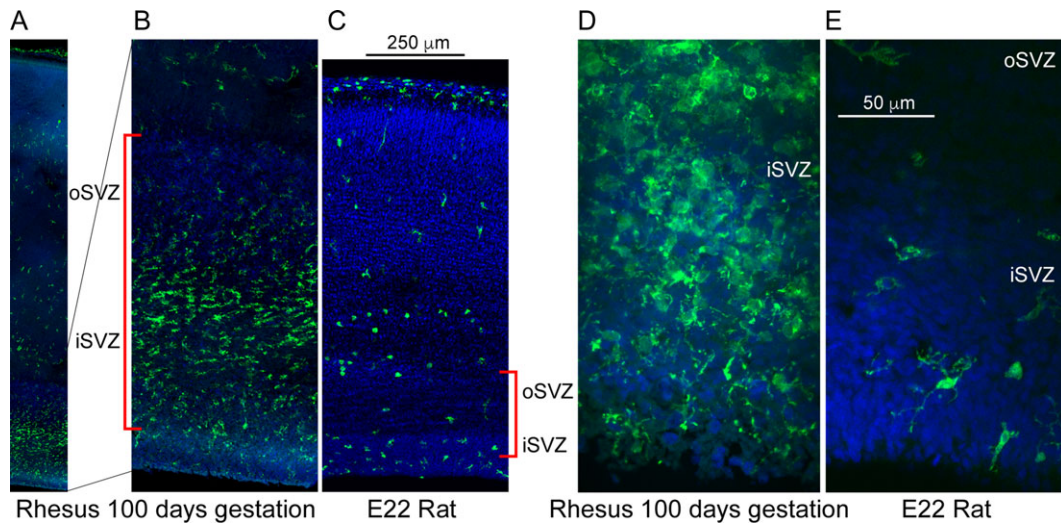


Figure 2. The density of microglial cells is higher in the proliferative zones of fetal rhesus monkey cerebral cortex than in the prenatal rat at the same relative stage of cortical development. (A) Distribution of microglial cells (green) in the fetal rhesus cerebral cortex in the second trimester (100 days gestation). (B) Same section at higher power highlights the density of microglial cells in the iSVZ and outer SVZ (oSVZ). (C) E22 rat neocortex shown at the same scale as panel B. In comparison, the density of microglia is much lower in the rat cortical proliferative zones at the same relative stage of cortical development. (D, E) Sections from the occipital cortex of the rhesus fetus in the second trimester (100 days gestation) and E22 rat highlight the dramatic difference in density of microglia between species. Microglial cell bodies and processes overlap in the fetal rhesus monkey, while individual cells can be visualized in the rat. Blue, DAPI.

Figure 3A (white arrow) was a typical example and had a pial fiber that extended over $300\mu\text{m}$ from the ventricle and was contacted by 6 Iba1+ microglial cells (asterisks, Fig. 3B).

The RG cell in Figure 3A, B (white arrow) was adjacent to 2 additional eGFP-labeled cells near the lateral ventricle (Fig. 3b1, white arrows). An Iba1+ microglia near the ventricle extended a large process that intercalated between the cells and was in apparent contact with the ventricular processes of the 3 eGFP+ RG cells (Fig. 3b1, white arrowhead). Microglia closely contacted RG cell pial fibers in a variety of ways. Some microglia interacted with pial fibers via large process extensions that partially wrapped the pial fiber (Fig. 3b3 and 3b4, white lines), and we noted that microglia often interacted with pial fibers in locations where enlargements or varicosities in the pial fiber were present (Fig. 3b3 and 3b4). We also noted microglia that had phagocytosed eGFP+ cellular elements, suggesting the pruning of eGFP+ cellular processes (Fig. 3b2). Microglia also extended processes that enveloped the fiber with a “handhold” appearance (Fig. 4A, open arrowhead), or extended multiple thin processes that encircled RG pial fibers (Fig. 4A, white arrowheads). We also observed microglia that resembled newborn cortical neurons migrating along pial fibers (Rakic 1972). These Iba1+ microglia extended a short leading process and were apposed to the RG cell pial fiber (Fig. 4B1–4B3).

To estimate the frequency of microglial cell contacts with RG cells, we traced the pial fiber of eGFP+ RG cells in $100\mu\text{m}$ thick sections ($N = 11$) and quantified the number of contacts. The RG cells had pial fibers ranging from 70 to $335\mu\text{m}$ long (average length $170 \pm 26.2\mu\text{m}^{\text{SEM}}$). Each pial fiber was contacted by $5.0 \pm 0.8^{\text{SEM}}$ microglial cells, and the interval between microglial cell contacts along the pial fiber averaged $34\mu\text{m}$. These data demonstrate a high frequency of contact points between microglia and RG cells in the cortical proliferative zones of the fetal rhesus monkey.

We tested whether cellular interactions between microglia and NPCs differed in injected versus noninjected tissues, or were influenced by eGFP expression. In cortical tissue obtained from control, age-matched fetal rhesus monkeys we labeled dividing

RG cells and their pial fiber with the 4a4 antibody (Noctor et al. 2002; Cunningham et al. 2013a), and costained tissue with Iba1. The 4A4 immunostaining labeled RG cells that were dividing at the surface of the lateral ventricle as well as their pial fibers. We observed the same cellular interactions between microglia and 4A4+ dividing precursor cells in control tissue that we noted in eGFP-expressing specimens: microglia directly contacted the pial fiber of proliferative RG cells (Fig. 4C), and some microglia gave the appearance of migrating along RG pial fibers (Fig. 4D1–D4).

Microglia Interact with IP Cells in Fetal Rhesus Monkey Cortex

In the second trimester of fetal monkey development, Tbr2+ IP cells are localized in a dense band in the iSVZ, a more diffuse band in the outer SVZ (oSVZ), and also sparsely populate the VZ (Martinez-Cerdeño et al. 2012). Microglia interactions with Tbr2+ and SVZ precursor cells occurred in each zone, and included contact, envelopment of cellular processes, and phagocytosis of entire cells. The microglial cell shown in Figure 5 (large arrowhead) extended reticulated processes that enveloped the ventricular contacting process and surrounded the soma of a Tbr2+ precursor cell in the VZ (Fig. 5, small arrowheads). The eGFP+ cell shown in Figure 6A (white arrow) was located in the iSVZ and had the morphological appearance of a migrating cell. It had a leading process $55\mu\text{m}$ long (small arrowheads) and a trailing process in contact with the pial fiber of its presumed RG parent cell. This cell expressed Pax6, but not GFAP (Fig. 6C,D). Iba1 immunostaining showed that microglia contacted the soma and enveloped the leading process of the migrating cell (Fig. 6B).

Periventricular Microglia Cells Contact NPCs at the Ventricle in Fetal Rhesus Monkey

We noted a novel microglial subtype in the VZ we termed periventricular microglial cells that were positioned at the surface of the ventricle or in the VZ close to the ventricle. Figure 6G and H show a microglial cell located on the surface of the

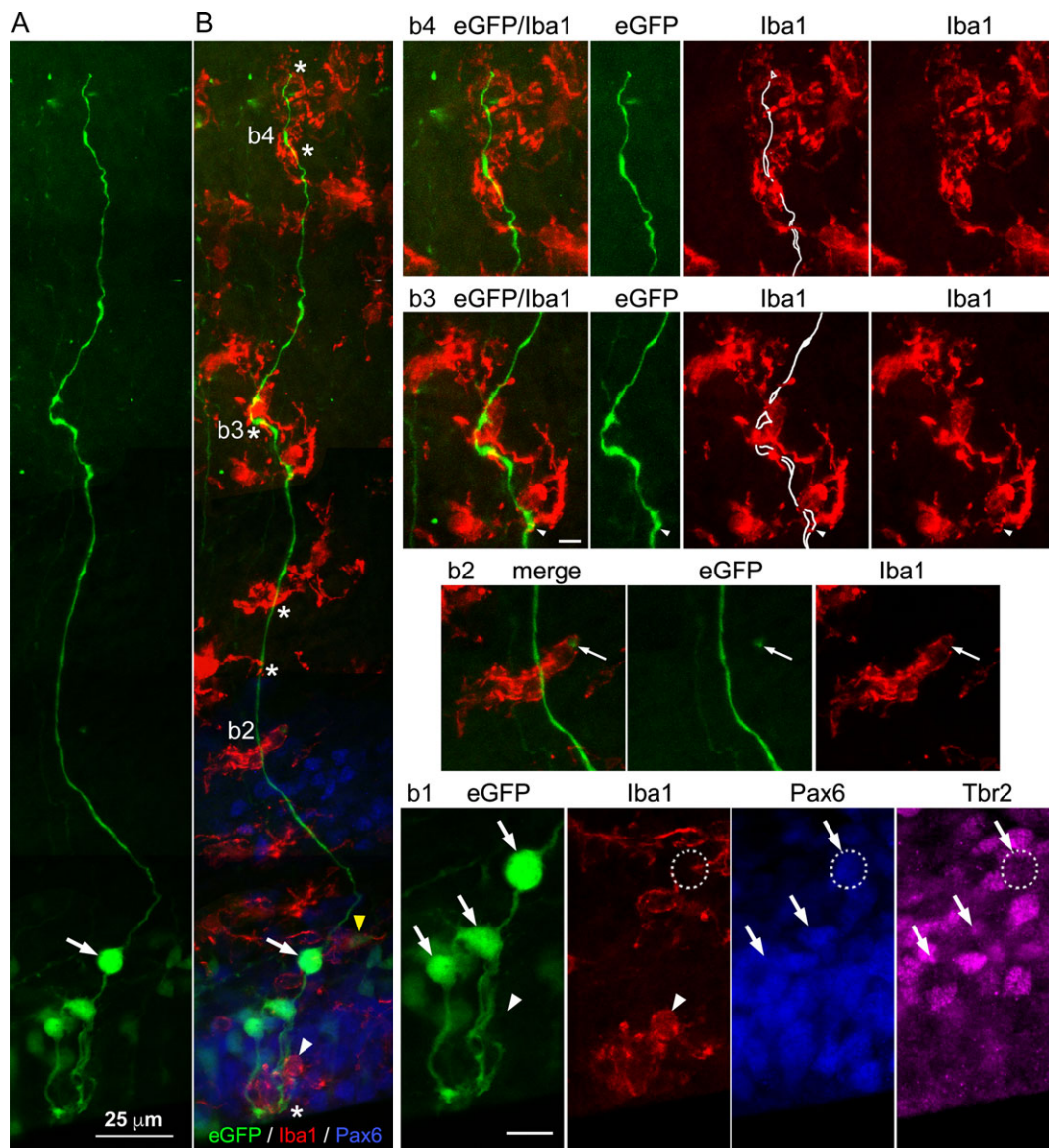


Figure 3. Microglial cells intimately interact with RG cells. (A) EGFP-expressing NPCs in the second trimester fetal rhesus cerebral cortex (5 days post-gene transfer). The eGFP+ RG cell (white arrow) had a pial fiber that coursed over 300 μm from the ventricle. (B) The section was triple immunostained with Iba1, Pax6, and Tbr2. Five Iba1+ microglia (red) directly contacted the pial fiber (white asterisks), and additional microglia included in the image were adjacent to but did not contact the pial fiber. (b1) The RG cell (white arrow, dotted circle) and neighboring eGFP+ cells (white arrows) expressed Pax6 (blue) but not Tbr2 (magenta). A microglial cell near the ventricular surface (white arrowhead) extended a large process that contacted and intercalated between the ventricular contacting processes of the eGFP+ VZ cells. (b2) Some microglia in the proliferative zones phagocytosed eGFP+ elements (white arrow), suggesting the pruning of eGFP+ cellular processes. (b3, b4) Microglial cells (red) often contacted pial fibers in locations where varicosities and enlargements were present. The microglia partially enveloped the pial fiber, creating an apparent groove or channel through which the pial process coursed (white lines). The scale bar in A = 25 μm applies to B. Scale bar in b1 = 10 μm applies to b1–b4.

lateral ventricle (large arrowhead) that contacted the apical surface of 3 eGFP-labeled precursor cells (Fig. 6G, H, small arrowheads; Supplementary Movie 3). This microglial cell may have contacted additional NPCs that were not labeled with eGFP.

We next examined the population of microglia within the VZ but located close to the ventricle. The periventricular microglia increased in number at later stages of neurogenesis as the microglial cell population in the cortex increased. The periventricular microglia appeared to be a distinct subset of microglia that were more ramified than microglial cells located in the SVZ and were often positioned approximately 10–30 μm from the ventricle,

extended elongated processes parallel to ventricle (Fig. 7A, large arrowhead), and contacted NPC processes (Fig. 7A, small arrowheads).

To better visualize periventricular microglia interacting with NPCs undergoing division at the ventricle, we examined microglia and mitotic NPCs at the surface of the ventricle in control specimens that preserved the ventricular surface. We stained the tissue with 4a4 to label mitotic NPCs, Iba1 to label microglia, and Pax6 or Tbr2 to label NPCs.

The ‘en face’ approach showed that many 4a4+ M-phase cells dividing at the ventricle were contacted by microglial cell processes (Fig. 7B, white arrows), including dividing NPCs that

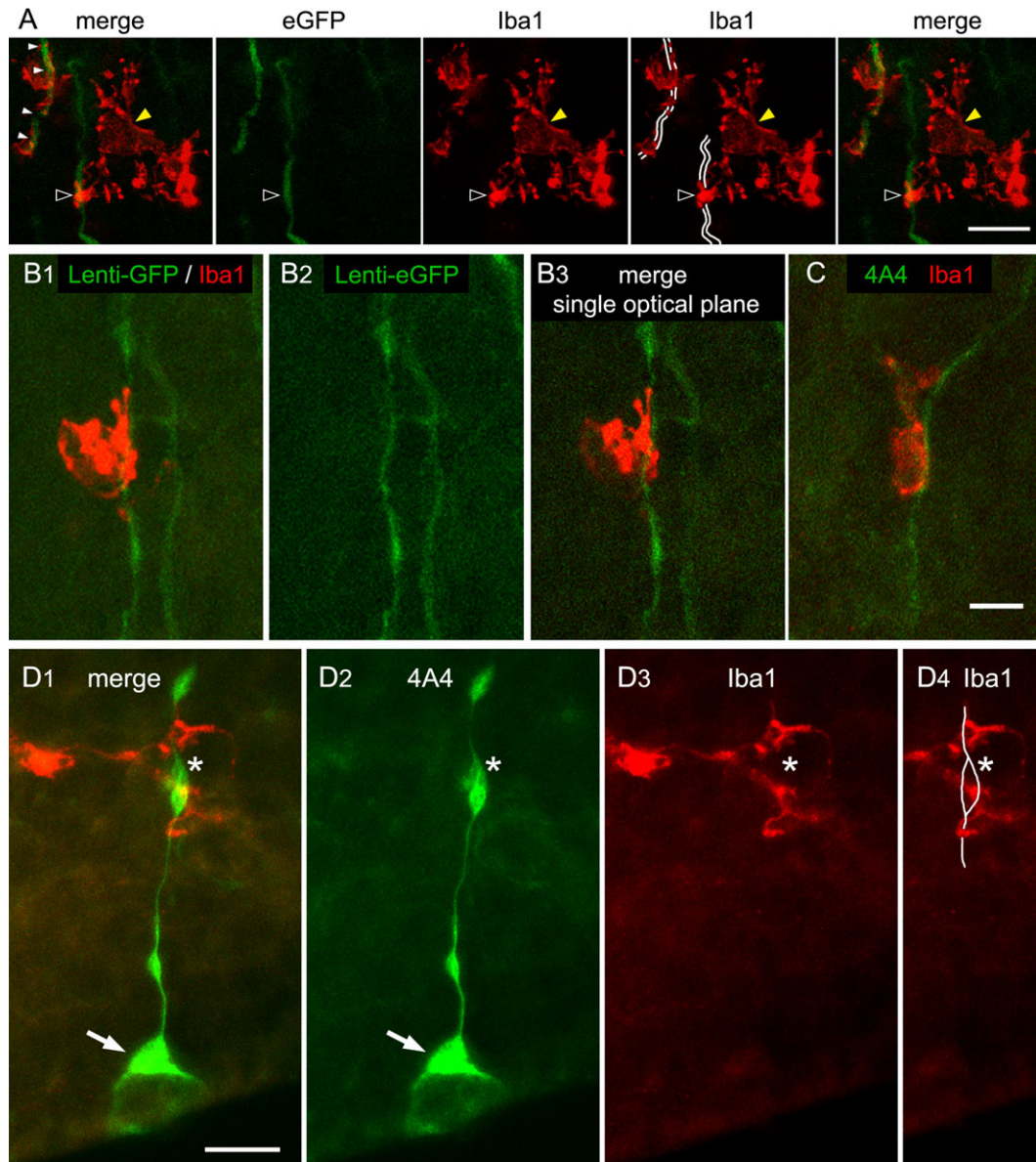


Figure 4. Microglia exhibit different forms of contact with the pial fibers of RG cells. (A) A microglial cell (red, yellow arrowhead) extended a process that contacts the pial fiber (green) via a “hand-hold” (open arrowhead), and other microglial processes encircled an adjacent pial fiber (white arrowheads). Left and right panels show same image for comparison with adjacent panels. (B₁-B₃) Some microglia appear to migrate along RG pial fibers. A microglial cell (red) is closely affiliated with an eGFP+ pial fiber (green). An Iba1+ microglial cell (red) is attached to the fiber. (B₃) Single optical plane shows close affiliation of the microglial cell (red) with the RG pial fiber (green). (C) Cortical tissue from control age-matched fetal monkey with stained Iba1 (red) and 4a4 (green) showed the same relationship between microglia and RG pial fibers in control animals. (D₁-D₄) Microglia contact pial fibers of mitotic RG cells in control animals. Fetal tissue from age-matched control monkey stained with 4a4 (green) and Iba1 (red) show microglial cell contact with the RG cell pial fiber. Microglia often contacted the pial fibers near enlargements and varicosities (asterisk). RG cell body indicated with white arrow. Scale bar in A = 10 μ m, C = 5 μ m, and D = 10 μ m.

expressed Tbr2 (Fig. 7B, yellow arrows). Microglial processes were located around the perimeter of 4a4+ cells, and in close contact with the 4a4+ NPC soma and processes. Some periventricular microglia extended thin processes that terminated on NPCs with a bouton-like terminal (Fig. 7B, white arrows; Supplementary Movie 4). The close, intimate contact between microglial cells and mitotic NPCs is consistent with the concept of functional interactions between these cell types.

EGFP+ Microglia Highlight NPC Contacts in Fetal Rhesus Monkey Proliferative Zones

Microglial cells were also labeled with eGFP. Most eGFP+ microglia were located in the VZ near the lateral ventricle as expected, but some were positioned hundreds of microns from the ventricle, suggesting they had migrated away after in utero lentiviral vector administration. EGFP-labeling of microglia confirmed that

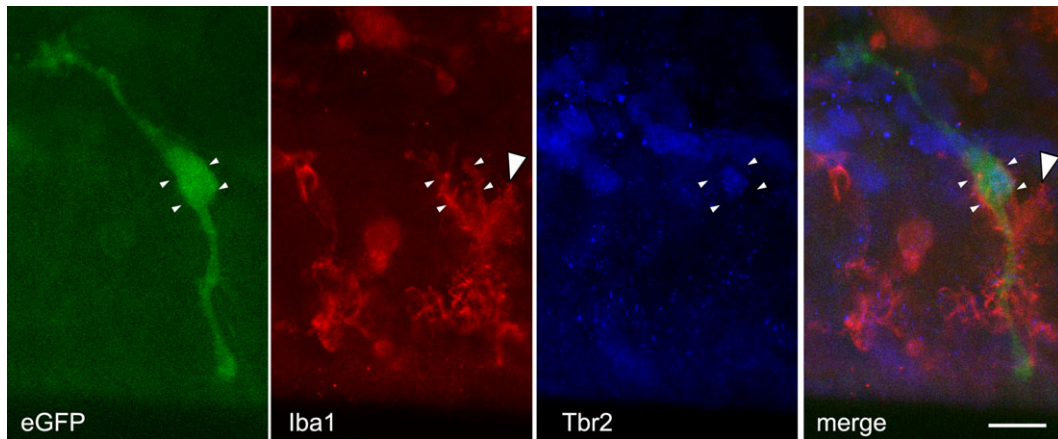


Figure 5. Microglia contact Tbr2+ cells in the VZ and SVZ. A microglial cell (red, large white arrowhead) enveloped an eGFP+ VZ precursor cell (green) that expressed Tbr2 (blue). The microglial cell extended reticulated processes that fully enveloped the ventricular contacting process and most of the soma (small white arrowheads) of the Tbr2+ cell. Scale bar = 10 μ m.

microglia near the ventricle contacted RG cell bodies while microglia in the SVZ contacted RG pial fibers. The data also showed that eGFP+ microglia were often in contact with eGFP+ NPCs. Figure 8 shows an eGFP+ RG cell with a pial fiber extending 250 μ m in the radial direction and parallel to the ventricular surface for an additional 50+ μ m. This pial fiber was contacted by 7 microglia (Fig. 8, white asterisks), one of which was eGFP+ (Fig. 8, white arrowhead). The RG cell expressed Pax6, but not Tbr2 (see Fig. 9C–G, white arrow), and included a Tbr2+ daughter cell apposed to the pial fiber (Fig. 9C–G, white arrowhead). The eGFP+ microglia contacting the pial fiber away from the ventricle had the complex activated morphology typical for microglia in the fetal monkey SVZ (Fig. 8, white arrowhead; Cunningham et al. 2013b). Confocal imaging confirmed that this eGFP+ cell expressed Iba1 and showed the contact point with the eGFP+ pial fiber (Fig. 9B).

An adjacent eGFP+ RG cell that was Pax6+ and Tbr2-negative (Figs 8 and 9C–G, yellow arrow) was contacted by an eGFP+ microglial cell near the ventricle (Fig. 9C–G, yellow arrowhead). This eGFP+ microglia contacted the ventricular process of the eGFP+ RG cell (Fig. 9D–F, yellow asterisk). These data highlight the variety and extent of contacts between microglia and NPCs.

Microglia in the Fetal Rhesus Monkey Cortex Simultaneously Perform Multiple Tasks

The morphology of many microglia in fetal monkey proliferative zones was difficult to discern through immunolabeling alone because of the cells' irregular shape and the high density and overlapping distribution of microglia in the fetal monkey VZ and SVZ (Fig. 2D). Figure 10 provides 3D perspective of an eGFP-labeled microglia to demonstrate the complex morphology and multiple interactions between microglia and surrounding NPCs. The image of the eGFP+ microglial cell produced from the full Z-series is shown at top (Fig. 10, row A) and subsequent rows show sequential subsets of optical planes in the Z-series (Fig. 10, rows B–E).

The first subset of optical planes in the Z-series (Fig. 10, row B) shows that the microglial cell (yellow arrowhead) phagocytosed a Tbr2+ cell (white arrow). The Tbr2-expressing nucleus was completely enveloped by the eGFP+ microglial cell. In the second subset of optical planes (Fig. 10, row C), the enveloped Tbr2+ nucleus remained visible and a phagocytic cup process contacting

a second Tbr2+ nucleus was visible (white arrows, Fig. 10, row C). The third subset of optical planes (Fig. 10, row D) showed the microglial cell (yellow arrowhead) extended a reticulated process that contacted the soma of an eGFP+ RG cells (Pax6+/Tbr2-negative, open arrowhead). EGFP expression highlighted reticulated processes that were difficult to visualize solely with Iba1-immunoreactivity (Fig. 10, row D, small yellow arrowheads). The eGFP+ microglial cell also extended a thin Iba1+ process in the opposite direction that contacted an eGFP+ cell at the ventricle (Fig. 10, row D, small white arrowheads). The final subset of optical planes (Fig. 10, row E) showed that the microglial cell contacted the ventricular process of a fifth precursor cell that expressed Pax6 (Fig. 10, row E, yellow asterisk). The RG contacted by the microglia in row D is indicated by the empty arrowhead. Together these panels show that this eGFP+ microglial cell simultaneously interacted with at least 5 NPCs in the VZ. This level of morphological complexity, with microglial cells directly contacting, enveloping, and phagocytosing multiple surrounding cells, simultaneously, was common in the fetal rhesus monkey telencephalon.

Discussion

Investigations in the developing brain have shown that microglia derive from yolk sac precursor cells (Ginhoux et al. 2010) begin to colonize the forebrain early in prenatal development (Andjelkovic et al. 1998; Rezaie and Male 1999; Verney et al. 2010; Toyoshima et al. 2012; Swinnen et al. 2013; Cunningham et al. 2013b; Arno et al. 2014) and are critical partners in key developmental processes (Schafer et al. 2012; Ueno et al. 2013; Squarzone et al. 2014; McCarthy and Wright 2017; Salter and Stevens 2017; Bilbo et al. 2018). However, the characteristics and functions of microglial cells in the developing brain are not yet fully understood.

In a previous study, we showed microglia phagocytose NPCs in the fetal cerebral cortex by labeling nuclear transcription factors specific to NPCs through immunostaining (Cunningham et al. 2013b). In the present study, we labeled NPCs in the fetal rhesus monkey with eGFP to gain a broader understanding of the cellular interactions between microglia and NPCs. We found that microglial cells make extensive contacts with NPCs throughout the VZ and SVZ and intimately interact with the RG scaffold. We noted that individual RG cells are contacted by multiple microglial cells at points from the ventricle through

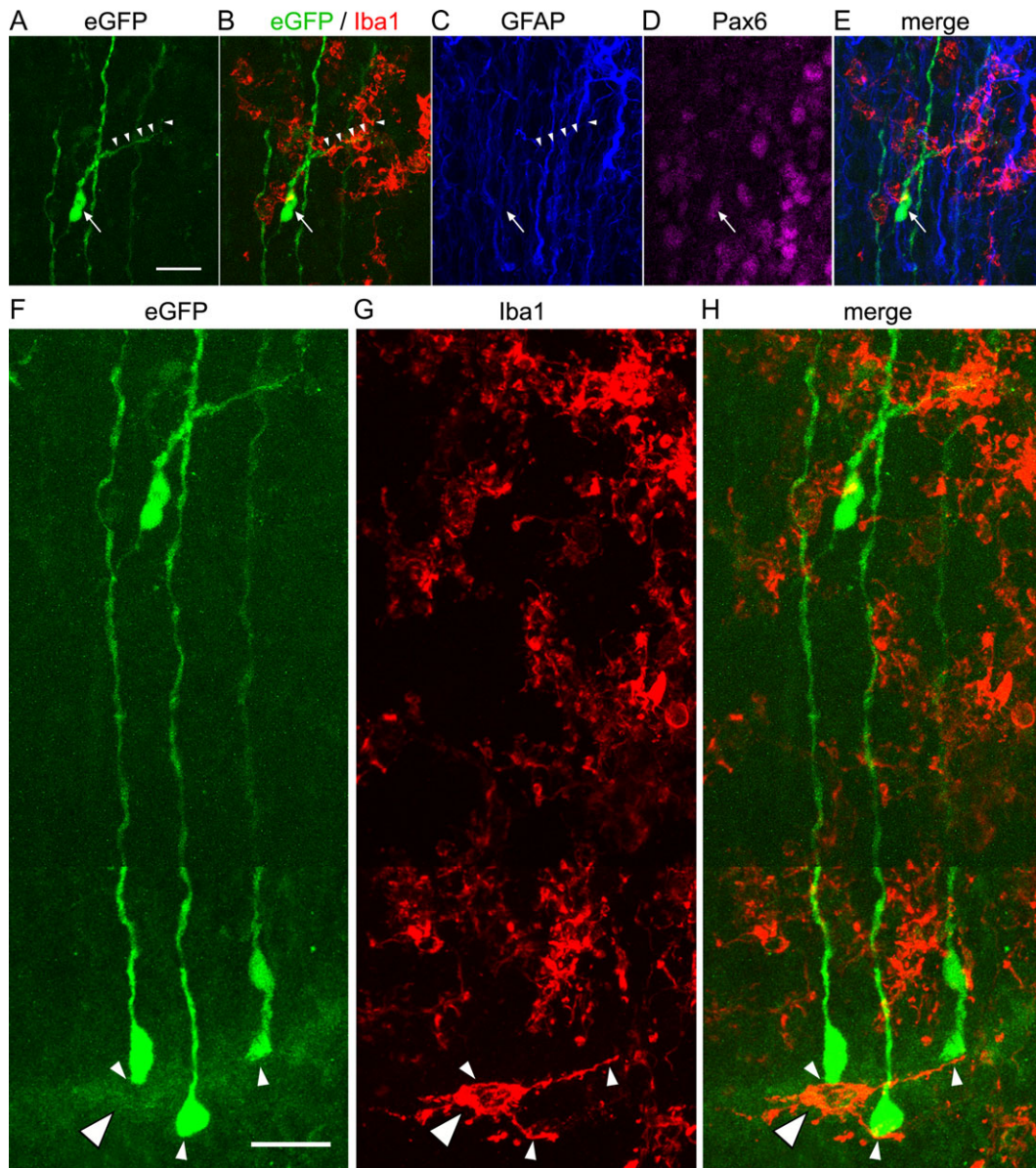


Figure 6. Microglia contact migrating cells in the SVZ. (A) An eGFP+ migrating daughter cell 200 μm from the ventricle in the SVZ (white arrow) from second trimester rhesus monkey (100 days; 14 days post-gene transfer). The daughter cell extended a leading process $\sim 55 \mu\text{m}$ long (white arrowheads) and a trailing process. (B) Merged panel showing intercellular relationships between eGFP+ pial fibers (green) and microglia (red). (C) The pial processes of the RG cells were GFAP+ (blue), but the migrating daughter cell did not express GFAP (white arrow, arrowheads). (D) The daughter cell expressed Pax6 (magenta). (E) Merged projection image. (F–H) Microglial cells contact NPCs at the ventricular surface. The panels show one microglial cell at the lateral ventricle (large white arrowhead) contacting the apical surface of 3 eGFP+ NPCs (small white arrowheads). Scale bars = 20 μm .

the proliferative zones, and that single microglial cells interact with multiple NPCs simultaneously. The ubiquity, variety, and complex nature of the interactions between these cell types suggest that microglia contribute to the regulation of NPC function in the developing brain.

Microglia in the Fetal Rhesus Cortical Proliferative Zones Display Complex, Activated Morphology

In the healthy adult cerebral cortex, microglial cells exhibit a “tiled” evenly spaced distribution with minimal overlap of processes between neighboring microglia. In contrast, microglia in the prenatal cerebral cortex are unevenly distributed; they sparsely populate the developing gray matter, densely populate

regions including the proliferative zones, and can overlap with neighboring cells. Furthermore, microglia in the fetal monkey cortex exhibit complex morphologies that, in the adult, would be classified as activated or typical for neuropathology. Microglial morphology in the fetal brain ranged from ameboid cells that lack detectable processes, to large cells with a few thick processes, to bipolar cells with elongated processes. In general, the morphology of microglia was associated with their location in the fetal cerebral cortex. For example, microglial cells in the SVZ often had large soma with short, thick processes (Fig. 2D), while microglia near the ventricle often elaborated long processes that extended parallel to the surface of the ventricle (Fig. 7A). Purinergic signaling has been shown to influence microglial morphology (Matyash et al. 2017). During early stages of cortical

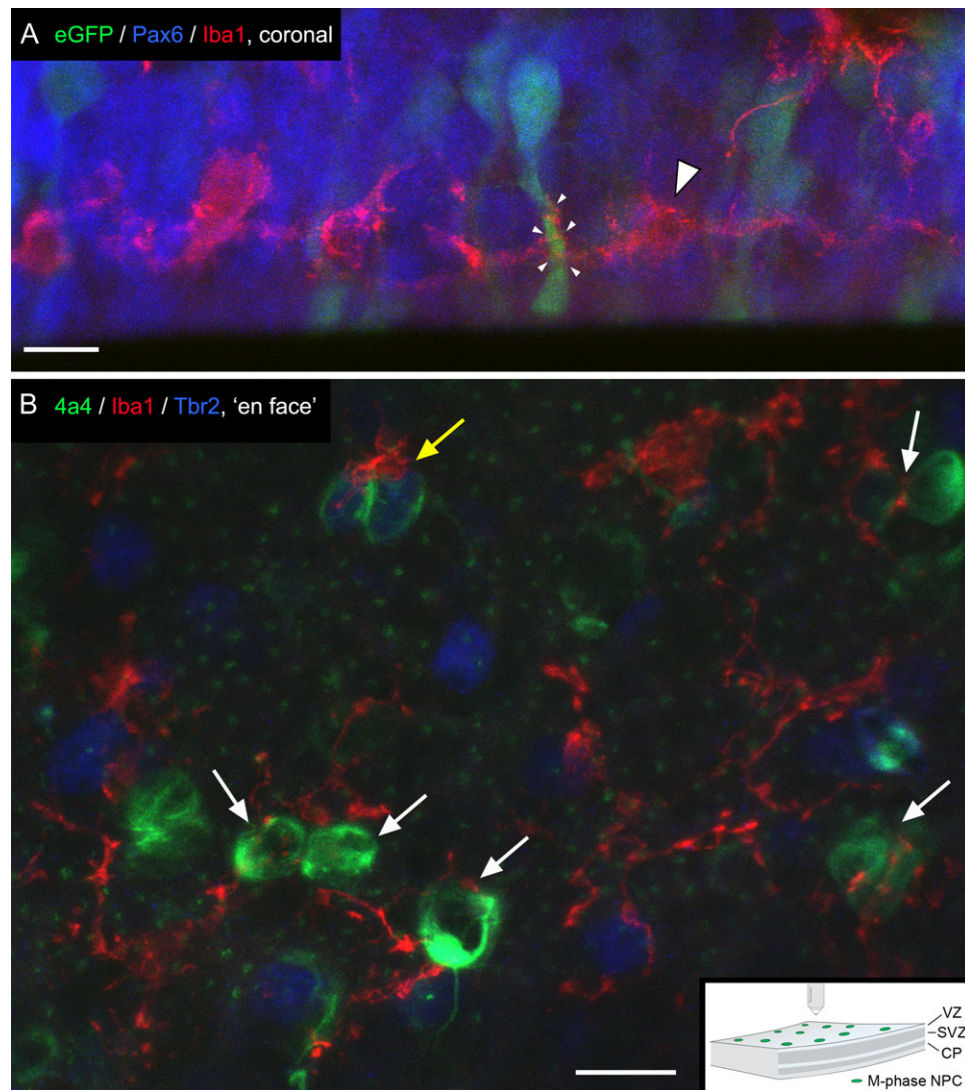


Figure 7. Periventricular microglia (red, white arrowhead) extend processes that are oriented parallel to the surface of the lateral ventricle. The periventricular microglia wrapped the ventricular contacting process of eGFP+ RG cells (small white arrowheads). (B) En-face view of the VZ in a control age-matched fetal rhesus monkey in the second trimester shows that microglia contact and closely interact with dividing NPCs at the surface of the ventricle. Most 4a4+ NPCs (green) dividing at the surface of the ventricle were contacted by processes of Iba1+ microglial cells (red). Some dividing NPCs expressed Tbr2 (blue, yellow arrow). Microglia also contacted Tbr2+ cells at the surface that were not dividing. Periventricular microglia had ramified processes that were thinner than microglia in the SVZ. Small green dots represent processes of interphase VZ cells. Inset at bottom right illustrates orientation of cortical tissue with dividing NPCs at the surface of the ventricle (green circles). CP, cortical plate. Scale bars = 10 μ m.

development, microglial morphology may also be influenced by the lack of an intact blood-brain barrier. Consistent with this idea, regions of the adult CNS that lack a blood-brain barrier, such as the pineal gland, are populated by microglia with a highly activated profile (Ibanez Rodriguez et al. 2016). The morphological phenotypes of microglia in the fetal monkey and rat cerebral cortices were similar, but we found that the density of microglia was much higher in the proliferative zones of the fetal rhesus monkey brain than embryonic rat in a volume per volume comparison (Fig. 2; Supplemental Movies 1 and 2). The increased density of microglia in primate versus rodent germinal zones may correlate with the significantly greater number of precursor cells in primates compared to rodents, and could also reflect closer interactions between microglia and NPCs in the primate brain.

Microglia Make Extensive Contacts with RG Cells and SVZ Cells in the Fetal Rhesus Monkey Cerebral Cortex

We observed numerous contact points between RG cells and microglial cells in the rhesus brain. Individual RG pial fibers were contacted by microglial cells on average every 35 μ m along the fiber. The contacts were not evenly spaced and often occurred where enlargements or varicosities were visible on the fiber (Figs 3 and 4). We were unable to determine which cell(s) initiated contact in fixed tissue sections, or how intercellular contacts may change over time. However, the potential for microglia to initiate contact with RG cells is supported by our time-lapse recordings showing predictable and constrained movements of RG cells and RG pial fibers over long periods of time (Noctor et al. 2001, 2004, 2008; Martinez-Cerdeño et al. 2012), compared to the

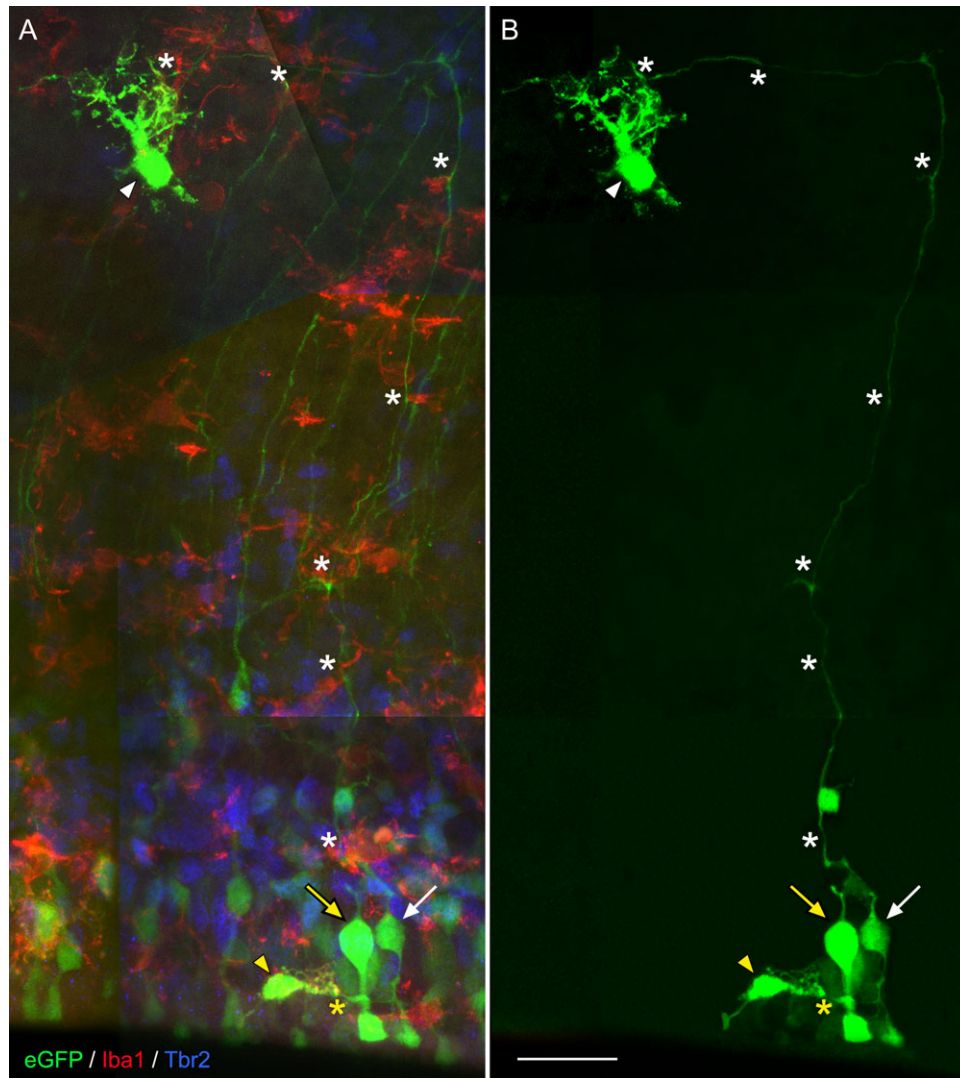


Figure 8. EGFP-expressing microglia often contact eGFP+ NPCs. eGFP+ microglial cells near the lateral ventricle (yellow arrowhead), and at a distance from the ventricle (white arrowhead) contacted eGFP+ RG cells. The microglial cell near the ventricle (yellow arrowhead) made contact close to the RG cell soma (yellow asterisk), and the microglial cell away from the surface (white arrowhead) contacted the RG pial fiber (white arrow). (A) Montage showing eGFP+ cells (green) in tissue immunostained for Iba1 microglia (red) and Tbr2 (blue). The RG pial fiber was contacted by 7 microglial cells (white asterisks). (B) Montage constructed by tracing a single eGFP+ pial fiber through each optical plane in a confocal Z-series. The pial fiber of the RG cell (white arrow) is contacted by an eGFP+ microglial cell 250 μm from the ventricle (white arrowhead). An adjacent eGFP+ RG cell (yellow arrow) is contacted by an eGFP+ microglial cell (yellow arrowhead) at the ventricle. Scale bar = 25 μm .

high motility of microglial cells (Dailey and Waite 1999; Davalos et al. 2005; Cunningham et al. 2013b), particularly in younger animals (Damani et al. 2011).

The morphology of the microglial contact with RG cells can be classified into 4 broad categories: 1) large membranous extensions that enveloped NPC soma (Fig. 10B, D); 2) phagocytic cups (Fig. 10C); 3) reticulated process extensions (Figs 5 and 10D); and 4) thin processes that enveloped RG pial fibers in the manner of a “hand-hold” (Fig. 4A), or that terminated on NPCs with a bouton-like terminal (Fig. 7B). We also observed microglia that appeared to migrate along RG pial fibers (Fig. 4B) in a manner reminiscent of neuronal migration (Rakic 1972). We did not detect a difference in the frequency of these types of interactions. These potentially distinct forms of contact between microglia and NPCs could represent stochastic processes, or may represent stages in a common sequence of cellular interactions. Alternatively, the distinct morphological forms of

microglial—NPC interactions could underlie distinct forms of cellular interactions, and the extension of process types may differ in response to specific stimuli. For example, ATP stimulates targeted process extension by microglial cells (Davalos et al. 2005; Hristovska and Pascual 2015). Proliferative cells in the VZ release ATP via hemichannels (Weissman et al. 2004), which may account for the microglial process extensions in the proliferative zones. Furthermore, specific forms of microglial extensions may represent a specialized form of membrane ruffling that is associated with cell pruning or phagocytosis (Ohsawa et al. 2000). In addition to contact points between microglia and RG cells, microglial cells also made extensive contacts with precursor cells in the SVZ. Of particular interest, we noted microglial cells closely interacting with the leading process of migrating daughter cells (Fig. 6A–E). Our data indicate that neuroimmune interactions may contribute to cellular migration in the fetal rhesus monkey cortex.

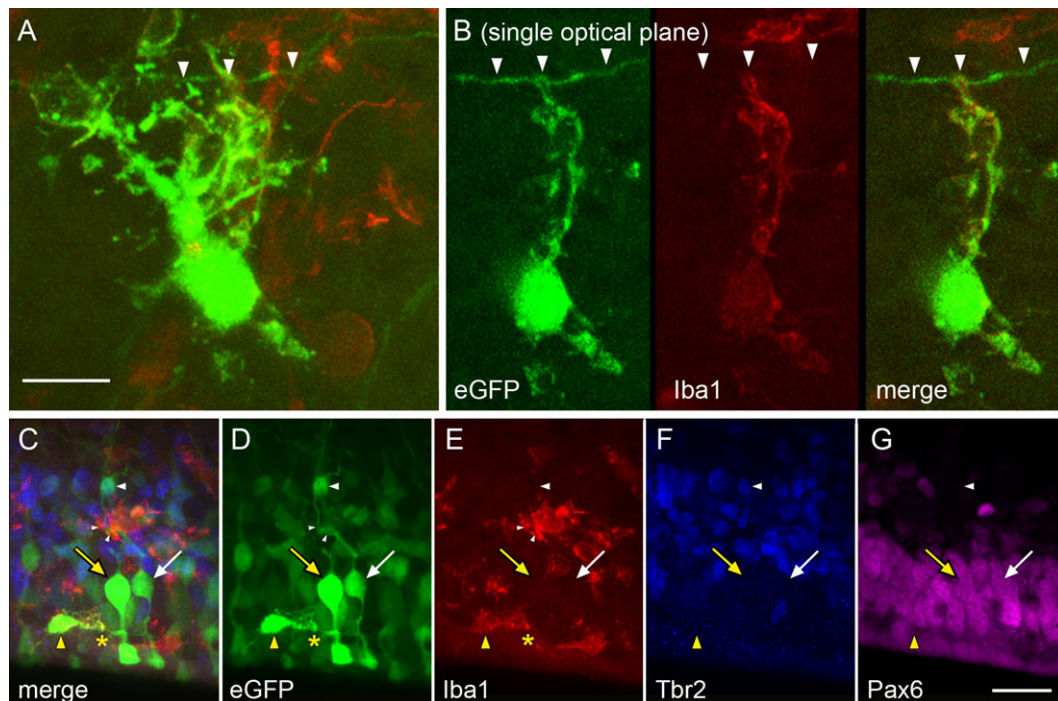


Figure 9. EGFP+ microglia affiliate with eGFP+ RG cells. (A) The eGFP+ microglial cell in the iSVZ shown in Figure 8. (B) Single optical plane shows the microglial cell contacted the RG pial fiber (white arrowheads) and expressed Iba1. (C-G) The RG cell on the right (white arrow) had a Tbr2+ daughter cell (white arrowhead), and a pial fiber that was contacted by the microglia shown in panel A. The RG cell on the left (yellow arrow) was contacted by an eGFP+ microglial cell near the ventricle (yellow arrowhead); contact point indicated by yellow asterisk. (D) EGFP expression; (E) Iba1 immunostaining. (F, G) Both RG cells expressed Pax6 (magenta) but not Tbr2 (blue). Scale bars = 10 μ m.

Microglial Cells Perform Multiple Tasks in the Fetal Rhesus Cerebral Cortex

EGFP-labeling showed that individual microglia closely interacted with multiple precursor cells simultaneously (Fig. 10). Cortical neurons synapse with thousands of neurons (Schuz and Palm 1989), and Bergmann glia in the cerebellum (Muller and Kettenmann 1995), and cortical astrocytes (Matyash and Kettenmann 2010) contact thousands of synapses that may include multiple cell types. Given the high connectivity between other cortical cell types, it is not surprising that microglia behave similarly.

The functional implications of contacts between fetal microglia and cortical NPCs are not yet understood, but the location and timing of these cellular interactions provide clues. During the stage of development that we analyzed in the second trimester fetal rhesus monkey, several developmental processes occur with respect to NPCs. Some RG cells continue to cycle in the VZ, undergoing divisions at the lateral ventricle that generate Tbr2+ IP daughter cells (Martinez-Cerdeño et al. 2012; Cunningham et al. 2013a). Many Tbr2+ IP daughter cells migrate to the SVZ, but some remain in the VZ and undergo divisions at the surface of the lateral ventricle (Fig. 7B). Some RG cells also delaminate from the ventricle and shift from the VZ to the SVZ by translocating the soma within the pial fiber, as shown in the rat (Noctor et al. 2004, 2008), human (Fietz et al. 2010; Hansen et al. 2010), monkey (Schmechel and Rakic 1979; Martinez-Cerdeño et al. 2012), and ferret (Voigt 1989; Reillo et al. 2011; Poluch and Juliano 2015; Wolf et al. 2017). Following the mass exodus of translocating RG cells, the VZ becomes significantly thinner and by the late second trimester (100 days gestation) the number of NPC divisions at the ventricle decreases significantly (Martinez-Cerdeño et al. 2012) and the neuroepithelium transforms into an

ependymal layer. How NPC delamination occurs is not yet fully understood. Microglial cells are known to perform homeostatic functions that include cellular pruning and phagocytosis (Kettenmann et al. 2011; Wolf et al. 2017). Our data show microglia positioned at the surface of the ventricle during a time when NPCs delaminate, and as the neuroepithelium transitions into an ependymal layer (Cunningham et al. 2013a), suggesting the possibility that microglia can facilitate the detachment of NPCs from the ventricular surface and function as structural modulators that play a role in remodeling the proliferative zones during late stages of neurogenesis. The proliferative zones in fetal rhesus monkey are significantly thicker than in rodents such as mice or rats (Smart et al. 2002; Fietz et al. 2010; Hansen et al. 2010; Martinez-Cerdeño et al. 2012). Consequently, the rhesus monkey proliferative zones likely require more extensive remodeling after precursor cells exit. This may be a factor in the larger microglial cell population in the rhesus monkey VZ and SVZ.

Implications for Developmental Neuropathology

The risk of inflammatory immune responses during prenatal development has become increasingly clear (Deverman and Patterson 2009; Meyer et al. 2009; Meyer 2013; Hagberg et al. 2012; Mattei et al. 2017; Salter and Stevens 2017; Wolf et al. 2017). Maternal influenza during the first trimester has been associated with neurodevelopmental disorders including autism (Brown et al. 2004; Hagberg et al. 2012), could potentially establish long-lasting elevated levels of microglial activation in the autistic neocortex (Morgan et al. 2010), and altered profiles of connectivity (Salter and Stevens 2017). These findings are consistent with the idea that maternal immune activation is a factor that can impact

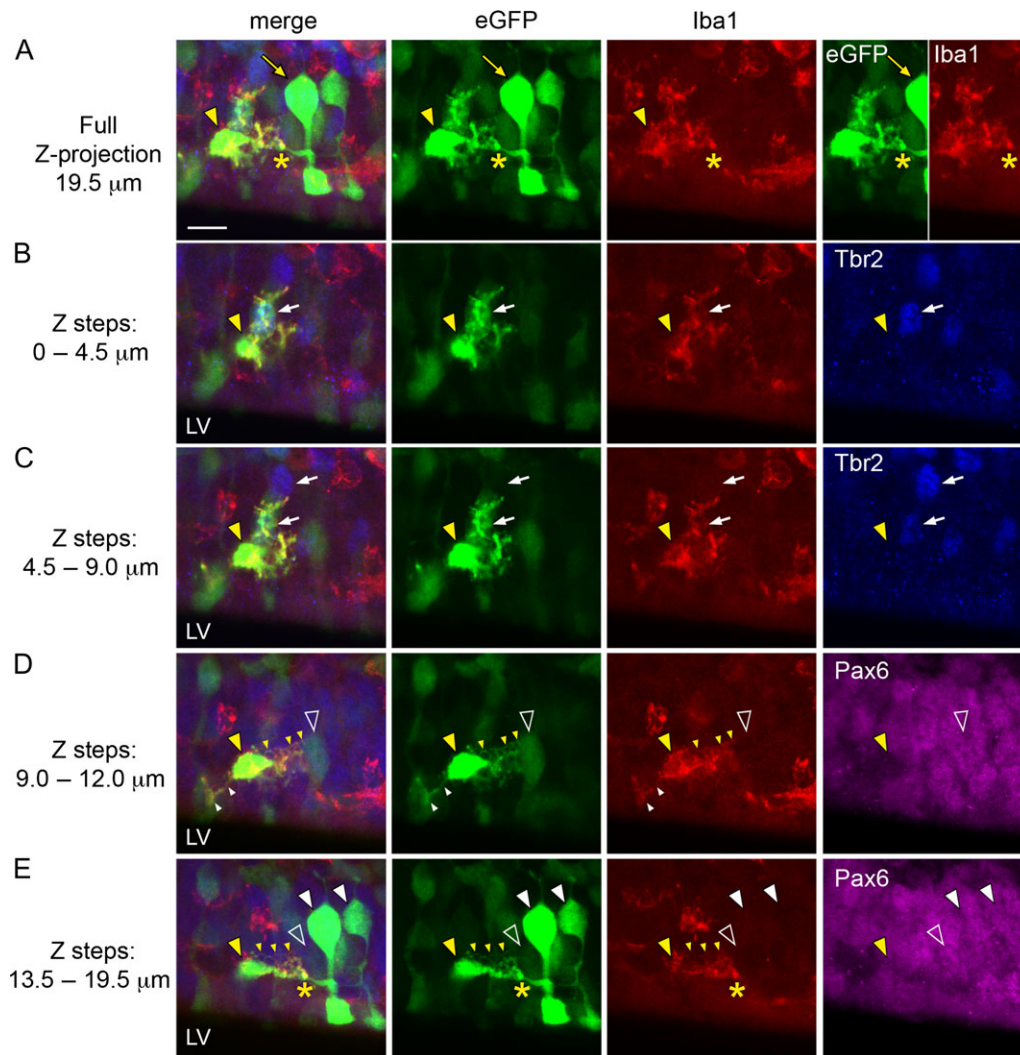


Figure 10. Microglial cells simultaneously perform multiple tasks: a single microglial cell contacted and/or phagocytosed 5 nearby precursor cells. (A) Projection image from the full Z-series shows the complex morphology of one microglial cell (yellow arrowhead). This cell expressed Iba1 and contacted (yellow asterisk) an adjacent eGFP+ RG cell (yellow arrow) and other VZ cells. (B) The first subset of optical plane images shows that the microglial cell phagocytosed a Tbr2+ cell (white arrow). (C) The second subset of optical planes shows that the same microglial cell extended a phagocytic cup in contact with a second Tbr2+ cell (white arrows). (D) The third subset of optical planes shows that the microglia extended a reticulated process (small yellow arrowheads) that contacted an eGFP+/Pax6+ RG cell (white arrowhead) and extended a process in the opposite direction that cradled the ventricular process of another eGFP+ RG cell (small white arrowheads). (E) The fourth subset of optical planes shows that the microglia (yellow arrowhead) made contact (yellow asterisk) with another eGFP+ RG cell that expressed Pax6 (white arrowheads). The eGFP+ RG cell contacted in row D is indicated with the empty white arrowhead. Scale bar in A = 10 μ m applies to all panels. LV, lateral ventricle.

the status and function of microglia in the developing cortex. Our data show extensive intimate contact between microglial cells and NPCs in the fetal rhesus monkey brain. The close nature of these interactions supports the concept of intercellular communication between the cells. These findings also strongly suggest that altering the function of fetal microglia directly by exposure to viruses or other pathogens can impact NPCs. The function and behavior of NPCs are complex, and include production of several daughter cell types (Shen et al. 2006; Noctor et al. 2008), molecular signaling with daughter cells (Yoon et al. 2008; Hansen et al. 2010; Shitamukai et al. 2011), and distinct migratory behaviors. Altering any of these functions could significantly change the timing or trajectory of normal developmental programs, set the stage for neuropathology, and could increase

susceptibility for disease later in life. Our previous data showing the temporal gradient in microglial colonization of the fetal primate SVZ (Cunningham et al. 2013b) may help explain the association between the timing of maternal immune activation and neuropsychiatric or neuropathological outcomes (Meyer et al. 2006). Precursor cells develop and function in a dense milieu that includes microglia; our current findings expand the repertoire of microglial cells to include monitoring, maintaining, and remodeling the neurogenic niche of the fetal primate cerebral cortex.

Supplementary Material

Supplementary material is available at *Cerebral Cortex* online.

Funding

These studies were supported by NIH grant MH101188 to S.C.N., the MIND Institute (IDDR; U54 HD079125), the Center for Fetal Monkey Gene Transfer for Heart, Lung, and Blood Diseases HL085794 to A.F.T., and the California National Primate Research Center base operating grant OD011107.

Notes

Conflict of Interest: None declared.

References

- Alliot F, Godin I, Pessac B. 1999. Microglia derive from progenitors, originating from the yolk sac, and which proliferate in the brain. *Brain Res Dev Brain Res.* 117:145–152.
- Andjelkovic AV, Nikolic B, Pachter JS, Zecevic N. 1998. Macrophages/microglial cells in human central nervous system during development: an immunohistochemical study. *Brain Res.* 814:13–25.
- Arno B, Grassivaro F, Rossi C, Bergamaschi A, Castiglioni V, Furlan R, Greter M, Favaro R, Comi G, Becher B, et al. 2014. Neural progenitor cells orchestrate microglia migration and positioning into the developing cortex. *Nat Commun.* 5:5611.
- Bilbo SD, Block CL, Bolton JL, Hanamsagar R, Tran PK. 2018. Beyond infection—maternal immune activation by environmental factors, microglial development, and relevance for autism spectrum disorders. *Exp Neurol.* 299:241–251.
- Brown AS, Begg MD, Gravenstein S, Schaefer CA, Wyatt RJ, Bresnahan M, Babulas VP, Susser ES. 2004. Serologic evidence of prenatal influenza in the etiology of schizophrenia. *Arch Gen Psychiatry.* 61:774–780.
- Chang WL, Tarantal AF, Zhou SS, Borowsky AD, Barry PA. 2002. A recombinant rhesus cytomegalovirus expressing enhanced green fluorescent protein retains the wild-type phenotype and pathogenicity in fetal macaques. *J Virol.* 76:9493–9504.
- Cooper AR, Patel S, Senadheera S, Plath K, Kohn DB, Hollis RP. 2011. Highly efficient large-scale lentiviral vector concentration by tandem tangential flow filtration. *J Virol Methods.* 177:1–9.
- Cunningham CL, Martinez-Cerdeño V, Noctor SC. 2013a. Diversity of neural precursor cell types in the prenatal macaque cerebral cortex exists largely within the astroglial cell lineage. *PLoS One.* 8:e63848.
- Cunningham CL, Martinez-Cerdeño V, Noctor SC. 2013b. Microglia regulate the number of neural precursor cells in the developing cerebral cortex. *J Neurosci.* 33:4216–4233.
- Dailey ME, Waite M. 1999. Confocal imaging of microglial cell dynamics in hippocampal slice cultures. *Methods.* 18:222–230. 177.
- Damani MR, Zhao L, Fontainhas AM, Amaral J, Fariss RN, Wong WT. 2011. Age-related alterations in the dynamic behavior of microglia. *Aging Cell.* 10:263–276.
- Davalos D, Grutzendler J, Yang G, Kim JV, Zuo Y, Jung S, Littman DR, Dustin ML, Gan WB. 2005. ATP mediates rapid microglial response to local brain injury in vivo. *Nat Neurosci.* 8:752–758.
- Deverman BE, Patterson PH. 2009. Cytokines and CNS development. *Neuron.* 64:61–78.
- Fietz SA, Kelava I, Vogt J, Wilsch-Brauninger M, Stenzel D, Fish JL, Corbeil D, Riehn A, Distler W, Nitsch R, et al. 2010. OSVZ progenitors of human and ferret neocortex are epithelial-like and expand by integrin signaling. *Nat Neurosci.* 13:690–699.
- Ginhoux F, Greter M, Leboeuf M, Nandi S, See P, Gokhan S, Mehler MF, Conway SJ, Ng LG, Stanley ER, et al. 2010. Fate mapping analysis reveals that adult microglia derive from primitive macrophages. *Sci.* 330:841–845.
- Hagberg H, Gressens P, Mallard C. 2012. Inflammation during fetal and neonatal life: implications for neurologic and neuropsychiatric disease in children and adults. *Ann Neurol.* 71:444–457.
- Hansen DV, Lui JH, Parker PR, Kriegstein AR. 2010. Neurogenic radial glia in the outer subventricular zone of human neocortex. *Nature.* 464:554–561.
- Hristovska I, Pascual O. 2015. Deciphering resting microglial morphology and process motility from a synaptic prospect. *Front Integr Neurosci.* 9:73.
- Ibanez Rodriguez MP, Noctor SC, Munoz EM. 2016. Cellular basis of pineal gland development: emerging role of microglia as phenotype regulator. *PLoS One.* 11:e0167063.
- Imai Y, Ibata I, Ito D, Ohsawa K, Kohsaka S. 1996. A novel gene *iba1* in the major histocompatibility complex class III region encoding an EF hand protein expressed in a monocytic lineage. *Biochem Biophys Res Commun.* 224:855–862.
- Kamei Y, Inagaki N, Nishizawa M, Tsutsumi O, Taketani Y, Inagaki M. 1998. Visualization of mitotic radial glial lineage cells in the developing rat brain by Cdc2 kinase-phosphorylated vimentin. *Glia.* 23:191–199.
- Kettenmann H, Hanisch UK, Noda M, Verkhratsky A. 2011. Physiology of microglia. *Physiol Rev.* 91:461–553.
- Martinez-Cerdeño V, Cunningham CL, Camacho J, Antczak JL, Prakash AN, Cziep ME, Walker AI, Noctor SC. 2012. Comparative analysis of the subventricular zone in rat, ferret and macaque: evidence for an outer subventricular zone in rodents. *PLoS One.* 7:e30178.
- Mattei D, Ivanov A, Ferrai C, Jordan P, Guneykaya D, Buonfiglioli A, Schaafsma W, Przanowski P, Deuther-Conrad W, Brust P, et al. 2017. Maternal immune activation results in complex microglial transcriptome signature in the adult offspring that is reversed by minocycline treatment. *Transl Psychiatry.* 7:e1120.
- Matyash V, Kettenmann H. 2010. Heterogeneity in astrocyte morphology and physiology. *Brain Res Rev.* 63:2–10.
- Matyash M, Zabiegalov O, Wendt S, Matyash V, Kettenmann H. 2017. The adenosine generating enzymes CD39/CD73 control microglial processes ramification in the mouse brain. *PLoS One.* 12:e0175012.
- McCarthy MM, Wright CL. 2017. Convergence of sex differences and the neuroimmune system in autism spectrum disorder. *Biol Psychiatry.* 81:402–410.
- Meyer U. 2013. Developmental neuroinflammation and schizophrenia. *Prog Neuropsychopharmacol Biol Psychiatry.* 42:20–34.
- Meyer U, Feldon J, Fatemi SH. 2009. In-vivo rodent models for the experimental investigation of prenatal immune activation effects in neurodevelopmental brain disorders. *Neurosci Biobehav Rev.* 33:1061–1079.
- Meyer U, Nyffeler M, Engler A, Urwyler A, Schedlowski M, Knuesel I, Yee BK, Feldon J. 2006. The time of prenatal immune challenge determines the specificity of inflammation-mediated brain and behavioral pathology. *J Neurosci.* 26:4752–4762.
- Morgan JT, Chana G, Pardo CA, Achim C, Semendeferi K, Buckwalter J, Courchesne E, Everall IP. 2010. Microglial activation and increased microglial density observed in the

- dorsolateral prefrontal cortex in autism. *Biol Psychiatry*. 68: 368–376.
- Muller T, Kettenmann H. 1995. Physiology of Bergmann glial cells. *Int Rev Neurobiol*. 38:341–359.
- Naldini L, Blomer U, Gage FH, Trono D, Verma IM. 1996. Efficient transfer, integration, and sustained long-term expression of the transgene in adult rat brains injected with a lentiviral vector. *Proc Natl Acad Sci U S A*. 93:11382–11388.
- Noctor SC, Flint AC, Weissman TA, Dammerman RS, Kriegstein AR. 2001. Neurons derived from radial glial cells establish radial units in neocortex. *Nature*. 409:714–720.
- Noctor SC, Flint AC, Weissman TA, Wong WS, Clinton BK, Kriegstein AR. 2002. Dividing precursor cells of the embryonic cortical ventricular zone have morphological and molecular characteristics of radial glia. *J Neurosci*. 22: 3161–3173.
- Noctor SC, Martinez-Cerdeño V, Ivic L, Kriegstein AR. 2004. Cortical neurons arise in symmetric and asymmetric division zones and migrate through specific phases. *Nat Neurosci*. 7:136–144.
- Noctor SC, Martinez-Cerdeño V, Kriegstein AR. 2008. Distinct behaviors of neural stem and progenitor cells underlie cortical neurogenesis. *J Comp Neurol*. 508:28–44.
- Ohsawa K, Imai Y, Kanazawa H, Sasaki Y, Kohsaka S. 2000. Involvement of Iba1 in membrane ruffling and phagocytosis of macrophages/microglia. *J Cell Sci*. 113(Pt 17):3073–3084.
- Paolicelli RC, Bolasco G, Pagani F, Maggi L, Scianni M, Panzanelli P, Giustetto M, Ferreira TA, Guiducci E, Dumas L, et al. 2011. Synaptic pruning by microglia is necessary for normal brain development. *Science*. 333:1456–1458.
- Poluch S, Juliano SL. 2015. Fine-tuning of neurogenesis is essential for the evolutionary expansion of the cerebral cortex. *Cereb Cortex*. 25:346–364.
- Rakic P. 1972. Mode of cell migration to the superficial layers of fetal monkey neocortex. *J Comp Neurol*. 145:61–83.
- Rakic P. 1974. Neurons in rhesus monkey visual cortex: systematic relation between time of origin and eventual disposition. *Science*. 183:425–427.
- Reillo I, de Juan Romero C, Garcia-Cabezas MA, Borrell V. 2011. A role for intermediate radial glia in the tangential expansion of the mammalian cerebral cortex. *Cereb Cortex*. 21: 1674–1694.
- Rezaie P, Male D. 1999. Colonisation of the developing human brain and spinal cord by microglia: a review. *Microsc Res Tech*. 45:359–382.
- Salter MW, Stevens B. 2017. Microglia emerge as central players in brain disease. *Nat Med*. 23:1018–1027.
- Schafer DP, Lehrman EK, Kautzman AG, Koyama R, Mardinly AR, Yamasaki R, Ransohoff RM, Greenberg ME, Barres BA, Stevens B. 2012. Microglia sculpt postnatal neural circuits in an activity and complement-dependent manner. *Neuron*. 74:691–705.
- Schmechel DE, Rakic P. 1979. A Golgi study of radial glial cells in developing monkey telencephalon: morphogenesis and transformation into astrocytes. *Anat Embryol*. 156:115–152.
- Schuz A, Palm G. 1989. Density of neurons and synapses in the cerebral cortex of the mouse. *J Comp Neurol*. 286:442–455.
- Shen Q, Wang Y, Dimos JT, Fasano CA, Phoenix TN, Lemischka IR, Ivanova NB, Stifani S, Morrissey EE, Temple S. 2006. The timing of cortical neurogenesis is encoded within lineages of individual progenitor cells. *Nat Neurosci*. 9:743–751.
- Shitamukai A, Konno D, Matsuzaki F. 2011. Oblique radial glial divisions in the developing mouse neocortex induce self-renewing progenitors outside the germinal zone that resemble primate outer subventricular zone progenitors. *J Neurosci*. 31:3683–3695.
- Smart IH, Dehay C, Giroud P, Berland M, Kennedy H. 2002. Unique morphological features of the proliferative zones and postmitotic compartments of the neural epithelium giving rise to striate and extrastriate cortex in the monkey. *Cereb Cortex*. 12:37–53.
- Squarzone P, Oller G, Hoeffel G, Pont-Lezica L, Rostaing P, Low D, Bessis A, Ginhoux F, Garel S. 2014. Microglia modulate wiring of the embryonic forebrain. *Cell Rep*. 8:1271–1279.
- Swinnen N, Smolders S, Avila A, Notelaers K, Paesen R, Ameloot M, Brone B, Legendre P, Rigo JM. 2013. Complex invasion pattern of the cerebral cortex by microglial cells during development of the mouse embryo. *Glia*. 61:150–163.
- Tang X, Falls DL, Li X, Lane T, Luskin MB. 2007. Antigen-retrieval procedure for bromodeoxyuridine immunolabeling with concurrent labeling of nuclear DNA and antigens damaged by HCl pretreatment. *J Neurosci*. 27:5837–5844.
- Tarantal AF. 2005. Ultrasound imaging in rhesus (*Macaca mulatta*) and long-tailed (*Macaca fascicularis*) macaques: Reproductive and research applications. In: *The Laboratory Primate*. Elsevier Ltd. pp. 317–352. DOI:10.1016/B978-012080261-6/50020-9.
- Tarantal AF, Skarlatos SI. 2012. Center for Fetal Monkey Gene Transfer for Heart, Lung, and Blood Diseases: an NHLBI resource for the gene therapy community. *Hum Gene Ther*. 23:1130–1135.
- Toyoshima Y, Sekiguchi S, Negishi T, Nakamura S, Ihara T, Ishii Y, Kyuwa S, Yoshikawa Y, Takahashi K. 2012. Differentiation of neural cells in the fetal cerebral cortex of cynomolgus monkeys (*Macaca fascicularis*). *Comp Med*. 62:53–60.
- Ueno M, Fujita Y, Tanaka T, Nakamura Y, Kikuta J, Ishii M, Yamashita T. 2013. Layer V cortical neurons require microglial support for survival during postnatal development. *Nat Neurosci*. 16:543–551.
- Verney C, Monier A, Fallet-Bianco C, Gressens P. 2010. Early microglial colonization of the human forebrain and possible involvement in periventricular white-matter injury of pre-term infants. *J Anat*. 217:436–448.
- Voigt T. 1989. Development of glial cells in the cerebral wall of ferrets: direct tracing of their transformation from radial glia into astrocytes. *J Comp Neurol*. 289:74–88.
- Weissman TA, Riquelme PA, Ivic L, Flint AC, Kriegstein AR. 2004. Calcium waves propagate through radial glial cells and modulate proliferation in the developing neocortex. *Neuron*. 43:647–661.
- Wolf SA, Boddeke HW, Kettenmann H. 2017. Microglia in physiology and disease. *Annu Rev Physiol*. 79:619–643.
- Yoon KJ, Koo BK, Im SK, Jeong HW, Ghim J, Kwon MC, Moon JS, Miyata T, Kong YY. 2008. Mind bomb 1-expressing intermediate progenitors generate notch signaling to maintain radial glial cells. *Neuron*. 58:519–531.
- Zufferey R, Nagy D, Mandel RJ, Naldini L, Trono D. 1997. Multiply attenuated lentiviral vector achieves efficient gene delivery in vivo. *Nat Biotechnol*. 15:871–875.